Original Article

Does baseline renal function always decrease after unilateral ureteral severe obstruction? —experimental validation and novel findings by Tc-99m diethylene triamine pentaacetate acid (DTPA) dynamic renal scintigraphy

Qisheng Yang[1,2], Changyin Wang[3], Chun Gao[4#], Wasili Maimaiti[4#], Shun Li[4#], Linglong Jiang[3], Meijuan Shen[3], Ying Shen[3]

[1]Emergency Center, [2]Department of Urology, [3]Department of Nuclear Medicine, Zhongnan Hospital of Wuhan University, Wuhan 430071, China; [4]Second Clinical Faculty, Medical School of Wuhan University, Wuhan 430071, China

[#]These authors contributed equally to this work.

Correspondence to: Changyin Wang. Department of Nuclear Medicine, Zhongnan Hospital of Wuhan University, No. 169 Donghu Road, Wuhan 430071, China. Email: changyinwang@rocketmail.com.

Background: There is a lack of consensus concerning changes in renal function after unilateral ureteral obstruction. The aim of this study was to assess the influence of ureteral obstruction on renal morphology and function and to explore the effectiveness of dynamic renal scintigraphy in evaluating obstructive renal function.

Methods: We established a model of right ureteral obstruction using New Zealand white rabbits. We measured the glomerular filtration rate (GFR) before the operation and from days 1 to 82 after obstruction, observed the changes in bilateral kidney sizes and the GFR, and then compared the differences between the left and right kidneys.

Results: The difference between left and right kidney sizes was not significant before obstruction (t=–0.430, P=0.674); the right kidneys increased in size after obstruction and were larger than the left kidneys (P≤0.001). Obstructed kidneys demonstrated a morphological process of decelerated expansion and retraction. The difference in GFR between the left and right kidneys was not significant before obstruction (t=1.77, P=0.098); during days 1–21 and 42–82 after obstruction, the GFR of the right kidneys decreased and was lower than that of the left kidneys (P<0.001); on day 28, the GFR difference between the left and right kidneys (t=1.62, P=0.130) and the difference in the right kidney GFR before and after obstruction (t=1.03, P=0.323) were not significant. The GFR of obstructed kidneys rapidly declined initially, experienced a tortuous process of repeated dormancies and multiple self-recoveries, and then gradually declined.

Conclusions: The GFR in hydronephrotic kidneys is fluctuating. Thus, evaluating the true function of hydronephrotic kidneys using only baseline GFR is difficult; however, combining baseline GFR with renal morphology to assess obstructive renal function and its recoverability can provide more meaningful results.

Keywords: Dynamic renal scintigraphy; glomerular filtration rate (GFR); hydronephrosis; kidney; ureteropelvic junction obstruction

Submitted Jan 06, 2019. Accepted for publication Jun 28, 2019.
doi: 10.21037/qims.2019.07.09
View this article at: http://dx.doi.org/10.21037/qims.2019.07.09

Introduction

Hydronephrosis is the most common urological disease, and ureteropelvic junction obstruction is a common cause of hydronephrosis (1,2). After unilateral ureteral partial obstruction, intrarenal pressure increases, and the renal pelvis and calyces further expand. Ureteral obstruction not only causes morphological changes in the kidneys but also affects their functions (2-6). The greatest hazard of obstruction is the resulting renal damage or even loss of renal function (2-6). The changes in renal function after obstruction remain controversial. Some scholars have found that renal function progressively declines in complete ureteral obstruction (3,4,6) and partial obstruction (7,8). Studies by Wang *et al.* (5) and Claesson *et al.* (9) showed that renal function drastically decreased in the early stage after partial obstruction and then tended to stabilize. These results indicate the importance of the timely removal of obstructions to prevent renal function damage. However, some academics have suggested that the glomerular filtration rate (GFR) of obstructed kidneys could remain at normal levels, even in adverse conditions (10-12). In clinical practice, other researchers have even observed the phenomenon of supranormal functions in hydronephrotic kidneys (13-17). Clearly, the results reported by scholars vary, but a comprehension of the characteristics of renal function damage after ureteral obstruction likely influences the treatment decisions of clinicians. Thus, clarifying the regularity of renal functional change after the ureteral obstruction has important clinical significance in correctly understanding the renal function results measured by dynamic renal scintigraphy, accurately evaluating the obstructed renal function and its recoverability, and making appropriate treatment decisions.

The GFR is an important parameter of renal function. In this study, we systematically observed morphological changes in obstructed kidneys and the regularity of renal functional changes. We found that the baseline GFR of obstructed kidneys presented changing features that differed from those described in the literature (3-6); moreover, we explored methods of evaluating the degree of impairment of obstructive renal function and predicting recoverability, as reported below.

Methods

Models of ureteral obstruction

This study was approved by the Animal Care and Use Committee of Wuhan University Center for Animal Experiments (AUP number: 2013110). Fifteen New Zealand white rabbits were provided by Wuhan University Center for Animal Experiments/ABSL-III Laboratory. All rabbits were healthy adult male animals over 8 weeks old and had normal renal function and body weight (range, 2.16–2.74 kg; mean: 2.51±0.17 kg). The animal models of right ureteral partial obstruction were established in accordance with the ureteral casing method (*Figure 1A*) (7). The rabbits were required to fast overnight and preoperatively. The hair on their backs was shaved using an electric pet hair clipper, and the rabbits were anaesthetized by intraperitoneal injection with 1% pentobarbital sodium in accordance with the standard of 30 mg/kg (pentobarbital sodium/body weight). After anaesthetization, experimental animals were fixed on a surgical platform in the prone position, disinfected and draped with medical towels, and then aseptic surgery was performed. An incision was made along the right side of the spine, and blunt dissection of the muscle tissues was performed; the ureter could then be found along the psoas muscle. After a portion of the ureter was dissociated, a polyethylene plastic pipe with a length of 1 cm and an inner diameter of approximately 0.8 mm was longitudinally cut open unilaterally. Then, the ureter was placed into the pipe approximately 1 cm below the ureteropelvic junction. The upper and lower ends of the plastic pipe were ligated and fixed with a silk thread such that the incision in the plastic pipe wall was closed. The ureter was replaced in the original position, and then the tissue and skin were sutured layer by layer (*Figure 1A*).

Instrument and conditions of dynamic renal scintigraphy

The instrument was a single photon emission computed tomography (SPECT) with a low-energy high-resolution collimator (Model #, e.cam; Siemens product, Hoffman Estates, IL, USA). The ^{99}Mo-^{99m}Tc generator was supplied by Beijing Atomic High-Tech Co., Ltd. Diethylene triamine pentaacetate acid (DTPA) was provided by Beijing Xinke Sida Pharmaceutical Technology Co., Ltd. For full syringe imaging and empty syringe imaging, the syringes were placed on a homogeneously thin board (γ-ray attenuation rate of the board was 6%), which was designed to immobilize experimental animals. The scanning conditions were as follows: (I) full or empty syringe imaging, matrix, 256×256; acquisition zoom, 1.0; acquisition time, 60 s. (II) Blood perfusion phase, matrix, 256×256; acquisition zoom, 2.67; acquisition time, 3 s/frame for a total of 20 frames.

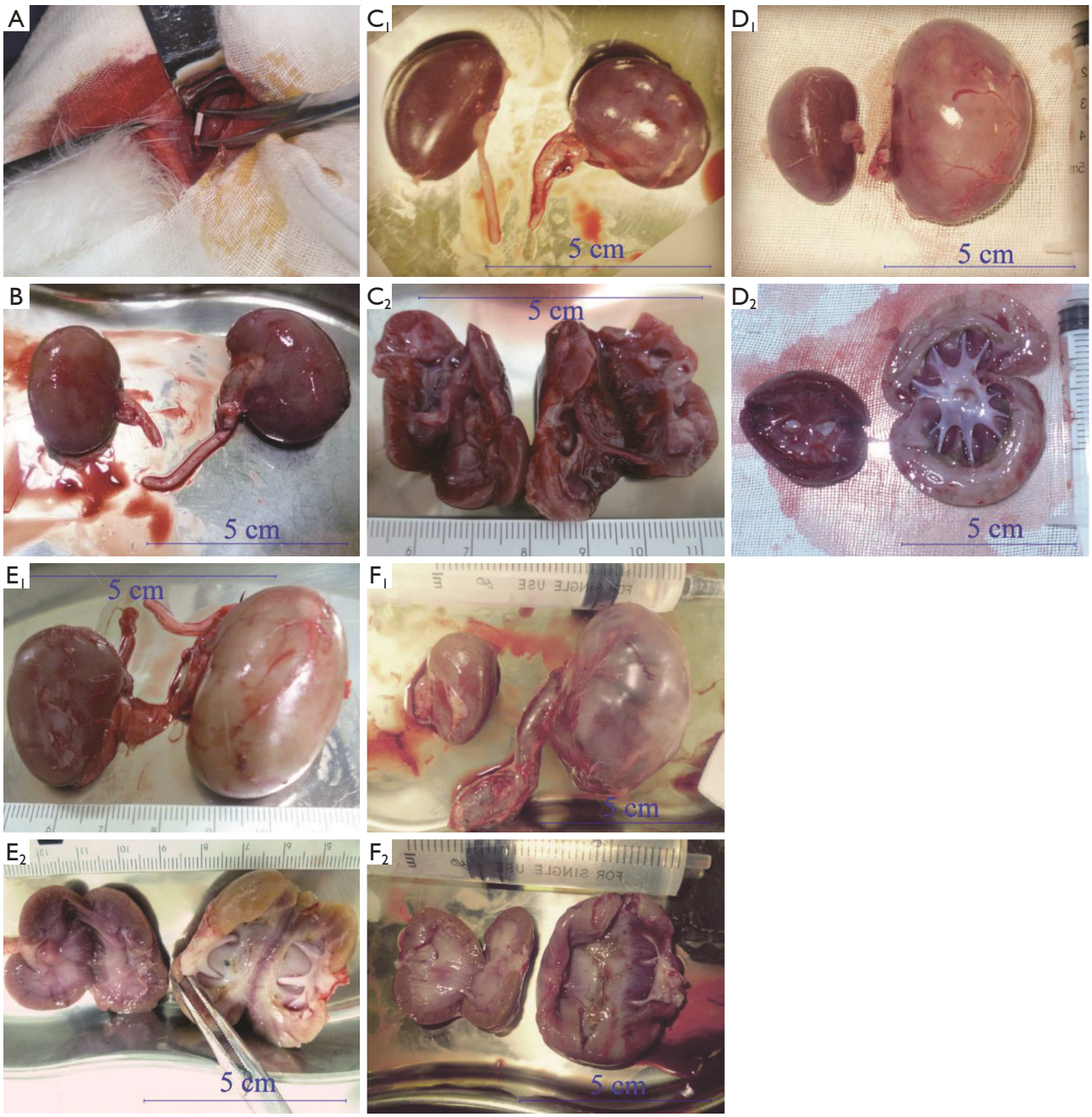

Figure 1 Comparison of gross specimens between hydronephrotic and normal kidneys. In (B,C,D,E,F), the left side of each figure is the left kidney, and the right side is the right kidney; (B,C_1,D_1,E_1,F_1) shows complete specimens, and (C_2,D_2,E_2,F_2) shows longitudinally dissected specimens; normal kidneys are brown. (A) Model of right ureteral obstruction. (B) On day 7 after obstruction, the right kidney swelled slightly and darkened. (C) On day 14, the right kidney swelled slightly, the renal parenchyma thickened slightly, and the sectional colour of the right kidney was similar to that of the left kidney. (D) On day 28, the right kidney was noticeably swollen, the renal parenchyma was markedly thickened, and the longitudinal section was lightly milky-white. (E) On day 56, the right kidney clearly was swollen, and the longitudinal section retracted and became lightly yellowish-white; the right renal parenchyma slightly thickened or presented a thickness similar to that of the left one, but the thickness was uneven. (F) On day 83, the right kidney was clearly swollen, but the renal parenchyma became significantly thin. The longitudinal section was noticeably shrunken and was a similar colour to the left kidney.

(III) Renal parenchyma phase, matrix, 256×256; acquisition zoom, 2.67; acquisition time, 10 s/frame for a total of 30 frames. The radiochemical purity of ^{99m}Tc-DTPA was greater than 95%.

Measurement of baseline glomerular filtration function

Experimental rabbits were required to be fasted overnight for over 12 h, and all residual food was removed from food dishes at 19:00 on the day before imaging was performed. The rabbits were allowed to drink water normally. At this time, the renal function of animals was at baseline. At 10 min before imaging, the animals were anaesthetized with 1% pentobarbital sodium according to the standard of 20 mg/kg (pentobarbital sodium/body weight) by intraperitoneal injection. When the gait of the animals became unstable, or the pinch-pressure response of animals showed a significant decrease, their limbs were quickly fixed on the designed thin board to prepare for scanning. Animals with inadequate anaesthetization were administered 20% of the previously injected dose to be further anaesthetized. To avoid the influence of deeply anaesthetizing the GFR, the animals that were deeply anaesthetized and could not show any response to pinch-pressure were observed for some time, and then scanning was performed when the pinch-pressure response first appeared. After a "bolus injection" of the imaging agent, ^{99m}Tc-DTPA, at approximately 3 mCi (0.2–0.5 mL), the acquisition program of dynamic renal scintigraphy was started immediately according to the above-mentioned scanning conditions.

Calculation of the GFR

An acquisition image of 2 to 3 min was selected to draw the region of interest (ROI). The renal ROI was outlined along functional kidney tissue, and the ampliative renal pelvis without function was not included in the renal ROI. GFR was calculated according to the Gates method (18) with the measured kidney depth.

Statistical analysis

Data were analysed with SPSS statistical software (version 22.0; IBM Corporation, Armonk, NY, USA). The data are presented as the mean ± standard deviation. Comparison between the left and right kidney sizes and comparison of kidney sizes before and after obstruction were performed with a paired *t*-test. A paired *t*-test was also used to compare the GFR between the left and right kidneys and the GFR before and after obstruction. The relationship between baseline GFR and kidney area size after obstruction and the relationship between baseline GFR after obstruction and obstruction duration were analyzed by Pearson correlation analysis. P values of less than 0.05 were considered indicative of statistical significance.

Results (*Figures 1-8*)

Morphological changes in the obstructed kidney

Normal kidneys of rabbits were brown, with a soft and flexible texture. The colour of the obstructed kidney gradually changed, the renal parenchyma swelled, and the renal texture gradually hardened (*Figure 1B*,*C*,*D*,*E*,*F*). In the late stage, the obstructed renal parenchyma was a light cream-white or yellowish-white colour (*Figure 1D*,*E*) and gradually became thin; at the end, the tangent plane colour of the obstructed kidneys partially recovered (*Figure 1F*). The obstructed kidneys experienced a change process of first expanding and then shrinking (*Table 1*).

Baseline GFR and GFR variation in obstructed kidneys

Before the obstruction, the bilateral renal GFR of rabbits was similar (*Figure 2*), and the difference in baseline GFR between bilateral kidneys was not significant (P>0.05) (*Table 2*). On day 28 after obstruction, the difference between bilateral kidneys was not significant (P>0.05), but at other time-points from days 1 to 82, the baseline GFR between bilateral kidneys was significantly different (P<0.001) (*Table 2*). After obstruction, the baseline GFRs of the left kidneys did not show any obvious change compared with those before obstruction, but those of the right kidneys presented an evident variation (*Table 2*). On day 28, the difference in right renal baseline GFR before and after the obstruction was not significant (P>0.05), but the differences were significant at other time-points (P<0.001) (*Table 2*). The baseline function of the obstructed kidney drastically declined in the early stage (*Figure 3*), then gradually rose (*Figures 4*,*5*), and even reached the same level as the contralateral kidney or the kidney before obstruction (*Figures 5*,*7A*,*B*,*C*). After reaching the peak, these levels gradually declined again (*Figure 6*).

Table 1 Comparison of bilateral kidney area sizes after right ureteral obstruction (mean ± standard deviation)

Obstruction time	Number of animals	Area of left kidney (mm^2)	Area of right kidney (mm^2)	Between right and left kidneys		Right kidney before and after obstruction	
				t	P	*t*	P
Before obstruction	15	851.4±72.2	844.3±79.7	–0.430	0.674	–	–
On day 1	15	854.6±99.9	1,019.8±160.5	6.217	<0.001	5.294	<0.001
On day 2	15	853.5±61.5	1,098.9±148.3	9.863	<0.001	6.984	<0.001
On day 3	15	835.2±67.9	1,120.0±222.2	6.028	<0.001	4.751	<0.001
On day 4	15	850.8±70.9	1,297.1±153.0	15.243	<0.001	9.581	<0.001
On day 5	15	895.6±63.8	1,375.4±175.3	12.263	<0.001	9.241	<0.001
On day 6	15	894.0±79.1	1,318.5±134.8	24.079	<0.001	11.689	<0.001
On day 7	15	871.1±40.1	1,373.6±132.8	18.828	<0.001	14.031	<0.001
On day 14	14	861.8±60.4	1,565.5±235.2	11.701	<0.001	9.793	<0.001
On day 21	13	854.0±79.0	1,665.5±293.1	11.061	<0.001	9.668	<0.001
On day 28	13	841.7±69.8	1,825.5±374.9	10.387	<0.001	9.228	<0.001
On day 42	10	877.2±83.1	2,000.7±497.9	7.991	<0.001	7.731	<0.001
On day 56	10	894.5±73.1	2,013.8±551.2	6.578	<0.001	7.058	<0.001
On day 68	9	913.8±60.5	1,818.6±457.4	6.648	<0.001	6.759	<0.001
On day 82	9	867.8±69.8	1,764.3±549.4	5.364	0.001	5.353	0.001

The relation between baseline GFR and kidney size in obstructed kidneys

Baseline GFR was positively correlated with the size of the renal long axis (r=0.237, P=0.007), short axis (r=0.384, P=0.000), and renal area (r=0.417, P=0.000) in healthy kidneys, but the correlations between baseline GFR and the size of the renal long axis (r=0.130, P=0.143), short axis (r=0.019, P=0.832), renal area (r=0.126, P=0.154), and renal pelvis area (r=0.169, P=0.066) in obstructed kidneys were not significant. In *Figure 8*, the changing course of the obstructed kidney was divided into eight stages according to baseline GFR.

Correlation between the baseline GFR of the obstructed kidney and duration of obstruction

The correlation between the baseline GFR of the healthy kidney and the duration of obstruction of the contralateral kidney was not significant (r=–0.005, P=0.955). The correlation between the baseline GFR of the obstructed kidney and duration of obstruction was also not significant (r=0.037, P=0.673). Clearly, the relationship between the baseline GFR of healthy or obstructed kidneys and duration of obstruction did not show unidirectional changing trends.

Discussion

From 1982 to 1984, Gates established a method of measuring the GFR and improved on it to make it more consummate (18-21). Subsequently, ^{99m}Tc-DTPA dynamic renal scintigraphy became a widely used technique in the quantitative evaluation of differential renal function (22-26). Our study showed that the GFR change in obstructed kidneys presented eight different stages, including a significant decline and self-recovery (*Figure 8A,B,C,D,E,F,G,H*).

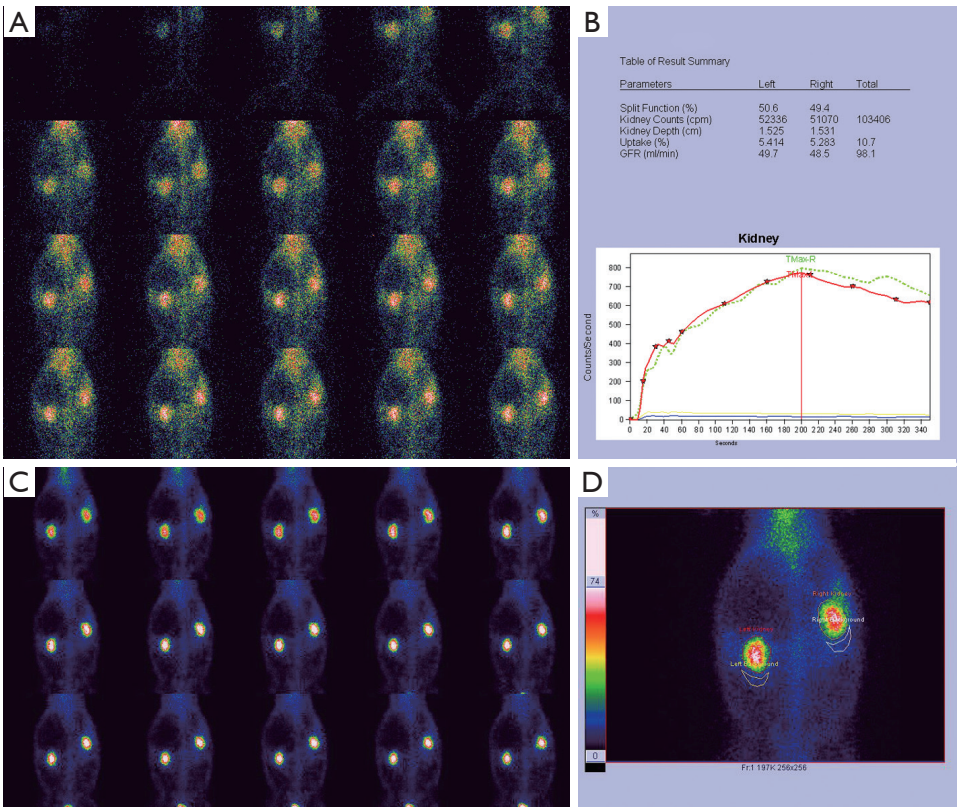

Figure 2 Dynamic renal scintigraphy findings of normal kidneys before ureteral obstruction. Notes: Images presented in *Figures 2-6* are of the same animal. (A) Blood perfusion phase; (B) renogram curves and GFR. The tendency of bilateral renal curves was similar. The GFR of the left kidney was 49.7 mL/min, and the GFR of the right kidney was 48.5 mL/min; (C) renal function phase; (D) drawing of renal ROI and background ROI. The blood perfusion, function, and radioactive change tendency of the bilateral kidneys were similar. GFR, glomerular filtration rate; ROI, region of interest.

The baseline GFR of obstructed kidneys dramatically decreased at the beginning stage and experienced two later dormant periods; the baseline GFR increased tortuously, the extent of the increase could be as high as, or even exceed, the level of GFR before obstruction, and then the GFR continually declined from the peak. This process is the regularity of obstructive renal GFR change after severe ureteral obstruction. In this study, the GFR of the obstructed kidneys neither progressively declined nor became stable after declining in the early stage and did not always maintain normal functional levels. Our findings are significantly different from those of the aforementioned researchers (3-12). The reason is that in our study, the observation time-points were more detailed and could fully reflect the changes in obstructive renal function, whereas the time-points of other researchers represented a fraction of ours and were not comprehensive. Our experiments observed GFR changes daily in the early stages of obstruction, while other experiments measured GFR only at weekly levels. Dissing *et al.* (12) measured GFR levels on the 4th week after obstruction and found unchanged renal function. In our study, the 4th week of obstruction was the highest peak time of GFR recovery, and the difference in obstructive renal function between this time-point and the period before obstruction was not statistically significant. In fact, the result of Dissing *et al.* (12) is consistent with our study at this time-point. Barthez *et al.* (10) found a self-recovering phenomenon of obstructive renal function after a decline, which was also similar to our study. Some studies missed the moment of maximum decline in the early stage of obstruction (4-6,27), which may be one of the reasons why the self-recovery of obstructive renal function was not found by these researchers.

The early GFR decrease in obstructed kidneys is

Table 2 Comparison between bilateral renal GFR after right ureteral obstruction (mean ± standard deviation)

Obstruction time	Number of animals	Total GFR (mL/min)	Left renal GFR (mL/min)	Right renal GFR (mL/min)	Between right and left kidneys		Right kidney before and after obstruction	
					t	P	*t*	P
Before obstruction	15	97.38±16.16	49.21±8.01	48.17±8.31	1.77	0.098	–	–
On day 1	15	65.05±13.63	50.40±8.31	14.65±7.87	15.85	<0.001	14.47	<0.001
On day 2	15	65.81±12.21	49.91±8.88	15.90±4.91	17.48	<0.001	17.89	<0.001
On day 3	15	68.13±10.95	50.94±8.69	17.19±3.87	16.72	<0.001	14.94	<0.001
On day 4	15	66.82±11.70	50.68±8.76	16.14±4.89	16.66	<0.001	20.23	<0.001
On day 5	15	68.49±11.99	50.29±8.46	18.20±5.08	17.41	<0.001	17.98	<0.001
On day 6	15	76.95±18.29	51.66±9.26	25.29±12.66	8.14	<0.001	7.73	<0.001
On day 7	15	84.37±16.30	51.90±8.60	32.47±9.96	8.38	<0.001	6.80	<0.001
On day 14	14	80.22±14.57	49.84±8.71	30.38±6.98	11.97	<0.001	10.04	<0.001
On day 21	13	80.25±14.57	49.23±8.74	31.02±10.38	10.47	<0.001	7.52	<0.001
On day 28	13	91.83±24.12	48.76±7.91	43.07±17.56	1.62	0.130	1.03	0.323
On day 42	10	68.57±18.78	48.33±9.08	20.24±10.98	12.20	<0.001	8.73	<0.001
On day 56	10	67.90±16.87	50.46±9.13	17.45±8.61	19.01	<0.001	17.36	<0.001
On day 68	9	65.08±19.08	48.11±9.52	16.98±12.71	7.88	<0.001	7.60	<0.001
On day 82	9	66.56±18.99	49.39±8.70	17.17±12.64	9.20	<0.001	9.66	<0.001

GFR, glomerular filtration rate.

regulated primarily by effective renal filtration pressure and is not mainly influenced by renal tissue injuries. After severe ureteral obstruction, the intrarenal pressure necessarily increases rapidly to a very high level (4,28), directly leading to a significant decrease in GFR. The continuous intrarenal high pressure causes kidney expansion, which is followed by a restorative increase in GFR as the intrarenal pressure gradually decreases from the peak level. The early decrease in obstructive renal function does not indicate irreversible glomerular damage. Zhao *et al.* (27) and Fink *et al.* (29) confirmed that renal function with complete ureteral obstruction could be restored to normal levels after the obstruction was removed in the 1st week after obstruction, which indicates that the early GFR decrease is reversible. In this study, the filtration function of obstructed kidneys rapidly declined at the beginning stage and then tortuously increased, demonstrating that the early decline was recoverable. In fact, the early GFR decrease indicates that renal function presents a dormancy in obstruction status and that the baseline function turns into a reserve function, resulting in a dramatic decline in baseline function and a corresponding increase in reserve function. This dormancy is unilateral and does not affect the contralateral kidney. The gradual increase in baseline GFR in obstructed kidneys from the lowest level is just the process showing that its reserve function is progressively activated in obstructed status. This activation is unilateral, progressive, and always accompanied by damage to renal function. Although the reserve function is fully initiated, and the baseline GFR is higher than that of the contralateral kidney (*Figure 7A,B,C*), the renal function in the protein load is significantly lower than that of the contralateral kidney (*Figure 7D,E,F*) and lower than its own function in the protein load before obstruction. After the reserve function is fully activated, its baseline renal function turns to a downward tendency. The duration of the peak value of the obstructive renal function

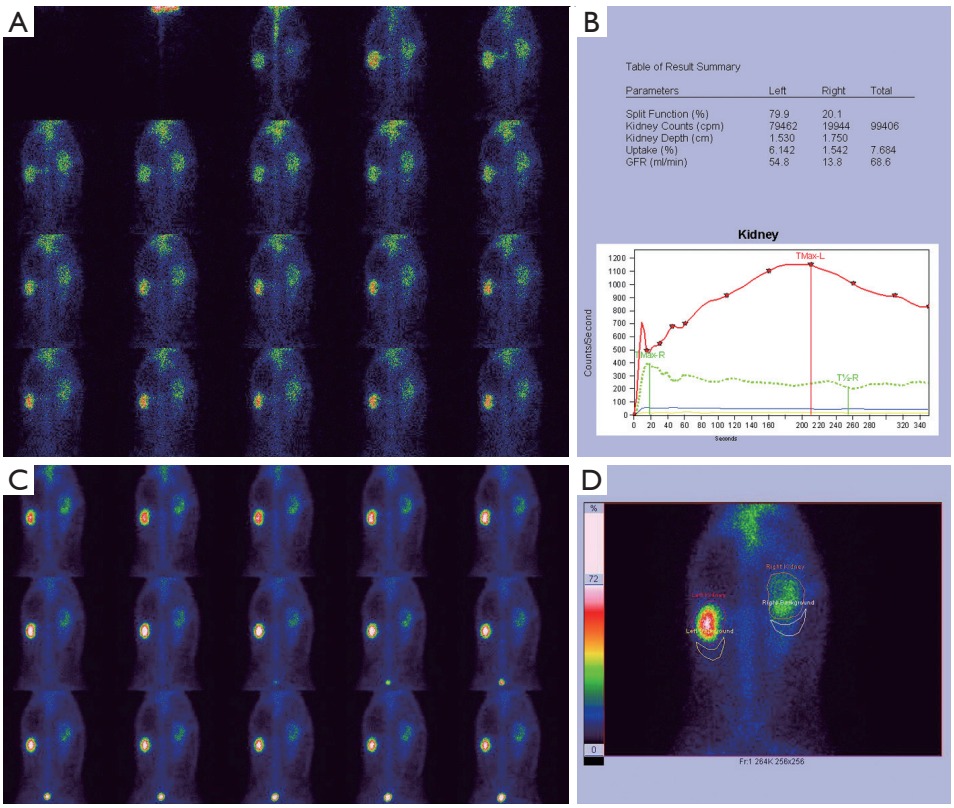

Figure 3 Results of dynamic renal scintigraphy on day 2 after right ureteral obstruction. Notes: Images presented in *Figures 2-6* are of the same animal. (A) Blood perfusion phase; (B) renogram curves and GFR; (C) renal function phase; (D) drawing of renal ROI and background ROI. The results show that the right kidney was slightly swollen and the renal pelvis was slightly expanded; right renal blood perfusion was slightly decreased, but the right GFR (13.8 mL/min) was noticeably decreased compared with the left GFR (54.8 mL/min). GFR, glomerular filtration rate; ROI, region of interest.

is rather short, and therefore, the normal or supranormal function of the obstructed kidney is uncommon in clinical practice. Ajmi *et al.* (13) reported a case with an increased function in hydronephrotic kidneys, and their reserve function was activated to peak as similarly described in this study. Moon *et al.* (14), Inanir *et al.* (15), and Khan *et al.* (16) thought that the supranormal functions in hydronephrotic kidneys were unlikely and were caused by artificial or technical reasons during the examination or image processing. However, Maenhout *et al.* (17) suggested that the supranormal function of the obstructed kidney was related to a hypofunction of the contralateral kidney. For a long time, we have always believed that the function of hydronephrotic kidneys cannot be accurately measured due to the influencing factors such as the kidney enlargement and the radioactivity of liver, spleen, and background. However, after carefully analyzing our experimental data, we found that this view can be put in doubt. In this study, we reveal the reasons for this rare clinical phenomenon from a new perspective. Clearly, it is a part of the evolution process of renal function following ureteral obstruction but cannot be reasonably explained by artificial or technical reasons or hypofunction of the contralateral kidney.

Under the condition of ureteral obstruction, the glomeruli, renal tubules, and renal interstitial frequently showed progressive changes, suggesting progressive damage to renal histology (5,8). However, the increased intrarenal pressure severely interferes with the parallelism between baseline GFR and the degree of glomerular damage and further interferes with the accuracy in determining renal tissue damage using baseline GFR. The true function of obstructed kidneys cannot be effectively assessed by baseline GFR. Therefore, determining the extent of functional impairment of hydronephrotic kidneys

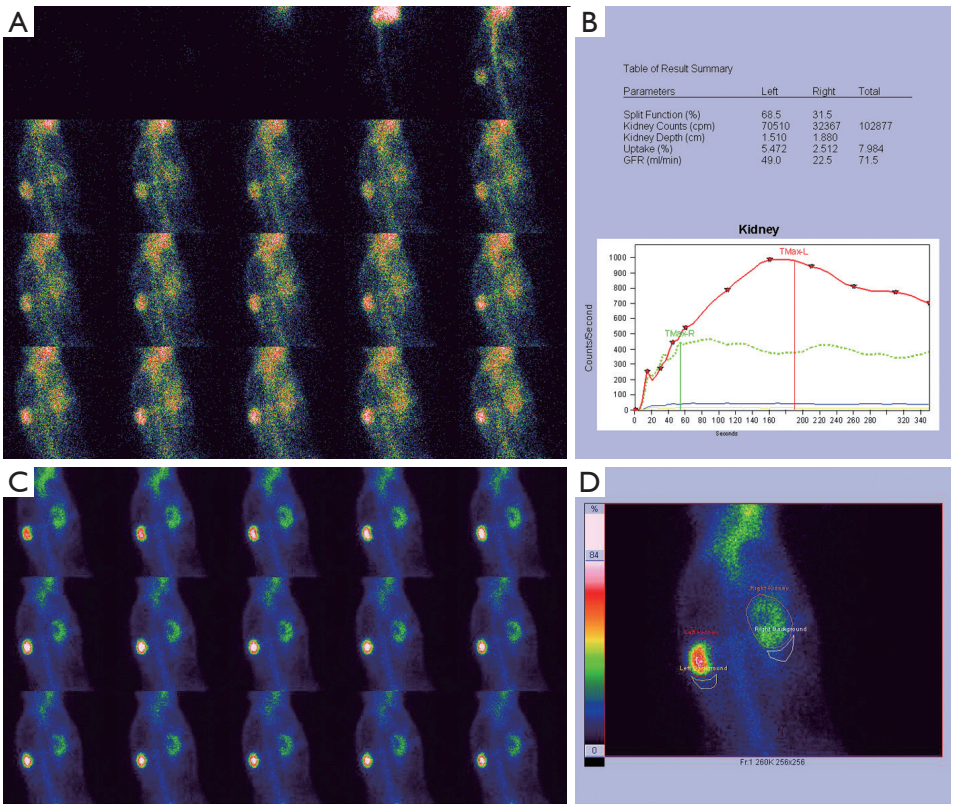

Figure 4 Results of dynamic renal scintigraphy on day 7 after right ureteral obstruction. Images presented in *Figures 2-6* are of the same animal. (A) Blood perfusion phase; (B) renogram curves and GFR; (C) renal function phase; (D) drawing of renal ROI and background ROI. The results show that the right kidney swelled and the renal pelvis expanded; right renal blood perfusion and GFR (22.5 mL/min) were clearly decreased in comparison with the left kidney (49.0 mL/min) but increased in comparison with the GFR (13.8 mL/min) on day 2 after obstruction. GFR, glomerular filtration rate; ROI, region of interest.

depending only on baseline GFR may lead to erroneous clinical decisions. When baseline GFR is drastically reduced, predicting the recoverability of obstructive renal function is of great importance. In fact, the necessity of predicting its recoverability is based on the inaccuracy of its measurement. If the measurement of the true function of the obstructed kidney is accurate, predicting the recoverability is unnecessary. We believe that the recovery ability of obstructive renal function is just the change in the magnitude of the increase in the routine measurement value of baseline GFR to its true renal function level. The key to predicting its recoverability is to evaluate its true function accurately. For accurately measuring the GFR of obstructed kidneys, excluding the interference of increased intrarenal pressure is the first countermeasure to consider. Parida *et al.* (30) reported a patient with transient obstruction at the ureteropelvic junction whose measurement value of renal function was very low at the first examination but increased significantly after the obstruction was relieved on its own. The fact suggests that if there is an opportunity to reduce the intrarenal pressure preoperatively, it is undoubtedly a good time to evaluate renal function. Aziz *et al.* (31) carried out percutaneous nephrostomy for hydronephrotic kidneys with less than 10% total renal function and observed an improvement of renal function. Therefore, percutaneous nephrostomy contributes to eliminating the influence of increased intrarenal pressure on GFR measurements and accurately evaluating the true function of the hydronephrotic kidney and its recoverability.

This study demonstrates different recoverability of GFR at different stages of obstruction. The analysis combining baseline GFR and kidney size contributes to the identification of obstruction stages. A considerable decline in baseline GFR can be found either in the early stage or the

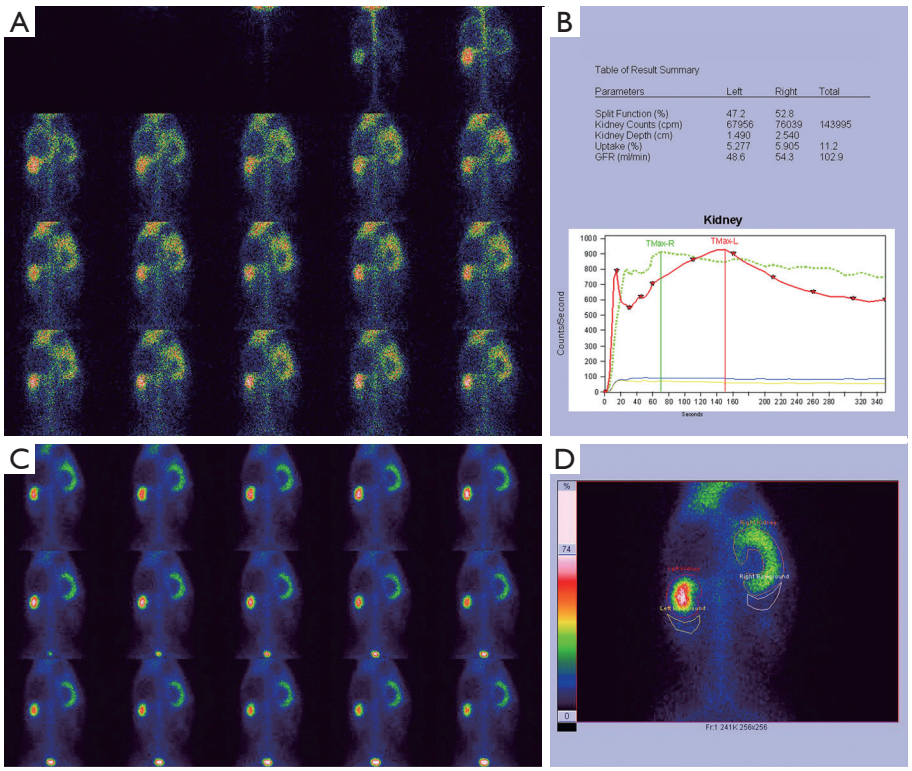

Figure 5 Results of dynamic renal scintigraphy on day 28 after right ureteral obstruction. Images presented in *Figures 2-6* are of the same animal. (A) Blood perfusion phase; (B) renogram curves and GFR; (C) renal function phase; (D) drawing of renal ROI and background ROI. The results showed that the right renal pelvis was noticeably expanded, right renal blood perfusion was slightly lower than that in the left kidney, right GFR (54.3 mL/min) was higher than left GFR (48.6 mL/min), and the right renal blood perfusion and GFR (54.3 mL/min) were further increased in comparison with the GFR (22.5 mL/min) on day 7 after obstruction. GFR, glomerular filtration rate; ROI, region of interest.

later period of obstruction, but the size of the obstructed kidney is significantly different between the early stage and the later period of obstruction. A substantial decrease in baseline GFR and a slight expansion in renal size imply that the obstructed kidney is in the early stage and has a better reserve function and recoverability. However, an obvious decline in baseline GFR and a severe expansion in renal size demonstrate that the kidney is in a later period of obstruction and has a poorer reserve function and no recoverability. Therefore, that we distinguish different obstructive stages by renal size is highly useful in estimating the true function of obstructed kidneys and predicting its recoverability.

Limitations

The first limitation is that during days 0 to 7 after ureteral obstruction, GFR measurements on the next day could be affected by a small amount of remaining renal radioactivity from the previous day. However, we routinely added local imaging before the examination to subtract residual radioactivity in the GFR calculation, so these effects were eliminated as much as possible. The second limitation is that excessive anaesthesia can affect the heart's hemodynamics and thus affect GFR, but it is difficult to perform GFR measurements at the same levels of anaesthesia. We tried to avoid excessive anaesthesia during the experiment. For those animals that had been deeply anaesthetized, GFR measurement was performed when there was an appropriate recovery. The third limitation is that we did not delve into the mechanism of baseline renal function changes after severe ureteral obstruction. The final limitation is that scars and severe adhesions had formed in the obstruction site. We failed to successfully remove the obstruction and observe the recovery of renal function.

The Gates method based on dynamic renal scintigraphy

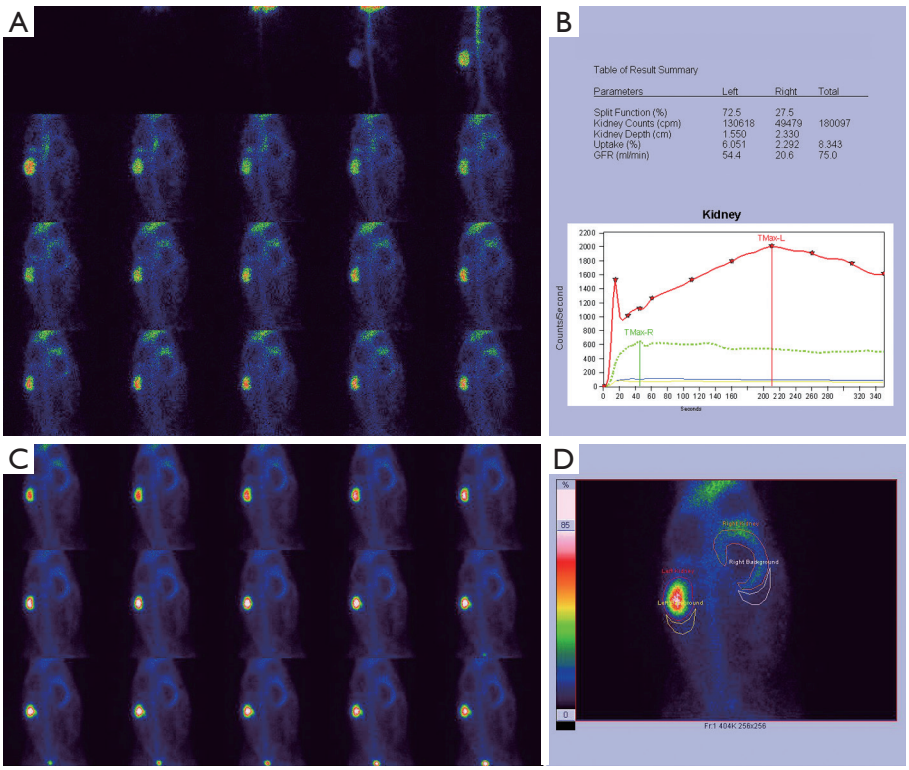

Figure 6 Results of dynamic renal scintigraphy on day 82 after right ureteral obstruction. The images presented in *Figures 2-6* are of the same animal. (A) Blood perfusion phase; (B) renogram curves and GFR; (C) renal function phase; (D) drawing of renal ROI and background ROI. The results show that the right renal pelvis noticeably expanded, and the right renal parenchyma became thin. The right renal blood perfusion and GFR (20.6 mL/min) were clearly lower than the left blood perfusion and GFR (54.4 mL/min) and were markedly decreased in comparison with the blood perfusion and GFR (54.3 mL/min) on day 28 after obstruction. GFR, glomerular filtration rate; ROI, region of interest.

also has some drawbacks. This method is a frequently used method for measuring GFR in humans in the clinic. It has obvious advantages in measuring split renal function, but its accuracy is affected by many factors. The Gates method was established a base on humans, and so has limitations for direct use in animal GFR measurements. In the Gates method, multiple estimation equations for kidney depth all were established based on the height and weight of the human body and thus is not suitable for animals. To avoid the inaccuracy of renal attenuation correction, we calculated the GFR using the measured kidney depth. The animal movement during scintigraphy may significantly affect the GFR accuracy. We not only closely observed the animal state when performing renal scintigraphy, but also paid attention to the rabbit movement during image analyses and performed the processing of motion correction. We re-performed a scintigraphic examination for rabbits on the next day if necessary. The Gates method is based on the 2–3 min renal uptake of ^{99m}Tc-DTPA to calculate GFR. Unlike humans, ^{99m}Tc-DTPA is sometimes discharged into the bladder during this period, which affects the accuracy and repeatability of renal uptake rate, and inevitably affects the GFR results. The studies by Kampa *et al.* showed that the 30–120 s renal uptake was appropriate for dog GFR calculations (32,33). However, we have not found a GFR calculation equation based on non-2–3 min renal uptake for experimental rabbits. In order to minimize the impact of this factor, we measured the bladder depth and calculated the bladder radioactivity, and then redistributed the bladder radioactivity back to the kidneys. The preoperative bladder radioactivity was equally allocated to the bilateral kidneys, and the postoperative bladder radioactivity was only allocated to the left kidney without hydronephrosis; the renal GFR was then calculated. Nonetheless, systemic bias

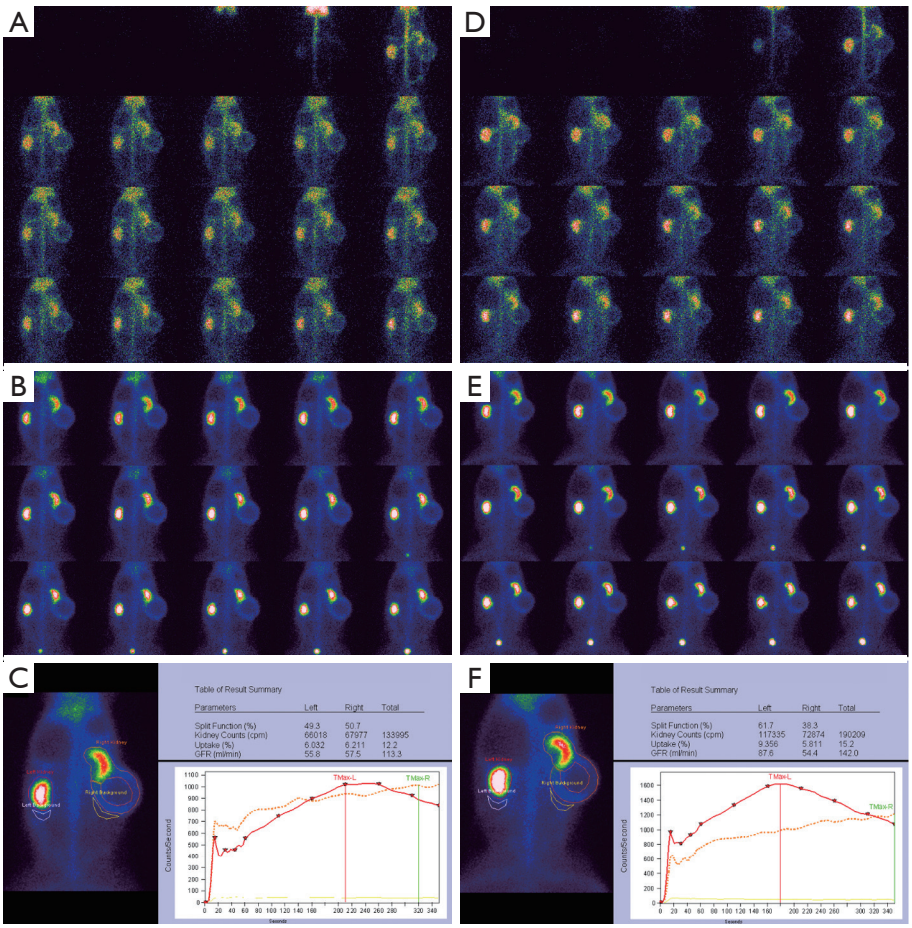

Figure 7 Dynamic renal scintigraphy in protein load and baseline status in right ureteral obstruction. An animal whose surgical incision split on day 28 after obstruction. (A,B,C) Dynamic renal scintigraphy at baseline status on day 68 after obstruction: (A) the phase of blood perfusion; (B) the phase of renal function; (C) the quantitative parameters and renogram curves. The GFR of the left kidney was 55.8 mL/min, and the GFR of the right kidney was 57.5 mL/min; (D,E,F) the dynamic renal scintigraphy in protein load on day 69 after obstruction: (D) the phase of blood perfusion; (E) the phase of renal function; (F) quantitative parameters and renogram curves. The GFR of the left kidney was 87.6 mL/min, and the GFR of the right kidney was 54.4 mL/min. The reserve function of the left kidney was 31.8 mL/min, and the reserve function of the right kidney was –3.1 mL/min. GFR, glomerular filtration rate.

may still exist due to the calculation of animal GFR using the Gates method. However, the trend of GFR changes was not affected. In addition, GFR based on dynamic renal scintigraphy is instantaneous GFR, while renal filtration is continuous, therefore, the GFR measured by Gates method also has certain limitations.

Conclusions

We established a pattern diagram of obstructive renal morphology and function, showing the tortuosity of baseline GFR changes and the inconsistency between baseline GFR and true GFR in ureteral obstruction. This study revealed that the supranormal function in the hydronephrotic kidney was caused neither by artificial nor technical factors nor by a hypofunction of the contralateral kidney. Rather, it was part of the evolutionary process of renal function following ureteral obstruction. Our study demonstrates that evaluating the true function of hydronephrotic kidney depending only on baseline GFR is difficult and underscores the importance of the combined use of renal morphology and baseline GFR in correctly understanding GFR results measured by

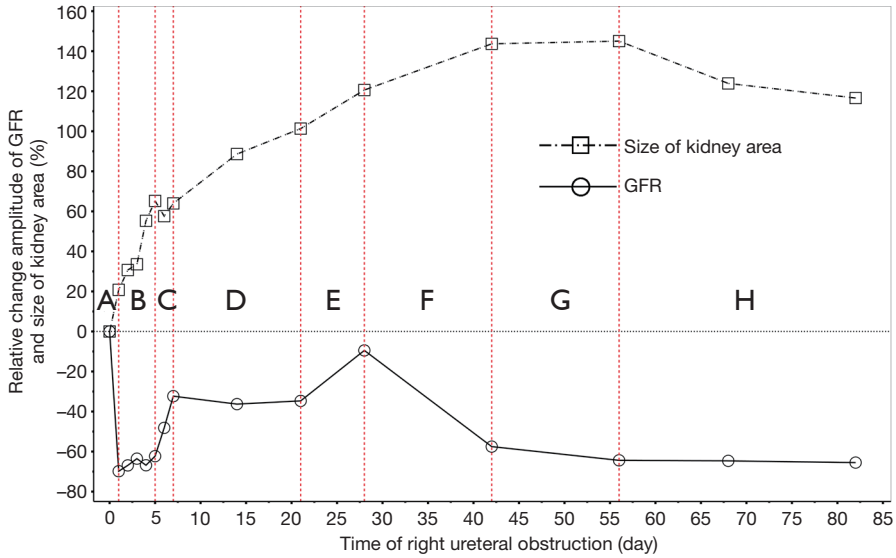

Figure 8 Relation between baseline GFR of obstructed kidney and renal area size. Relative change amplitude of renal area size (%) = [(S_b–S_a) ÷S_a] ×100, where Sa is the size of the renal area before obstruction, and Sb is the size of the renal area after obstruction. The units of both are mm^2. Relative change amplitude of renal GFR (%) = [(GFR_b – GFR_a) ÷ GFR_a] ×100, where GFR_a is the GFR before obstruction, and GFR_b is the GFR after obstruction; the units of both are mL/min. (A) The beginning stage of obstruction; (B) the stage of early dormancy; (C) the rapidly rising stage of the early period; (D) the stage of mid-term dormancy; (E) the slowly rising stage of the middle period; (F) the rapidly declining stage of the later period; (G) the slowly declining stage of the later period; (H) the stage of renal retraction. GFR, glomerular filtration rate.

dynamic renal scintigraphy and predicting the recoverability of obstructive renal function.

Acknowledgments

We thank Yueling Yang, Fen Wang and other staff of Wuhan University Center for Animal Experiment/ABSL-III Laboratory for animal management.
Funding: This work was supported by the Natural Science Foundation of Hubei Province of China (grants No. 2011CHB035).

Footnote

Conflicts of Interest: The authors have no conflicts of interest to declare.

Ethics Statement: This study was approved by the Animal Care and Use Committee of Wuhan University Center for Animal Experiments (AUP number: 2013110).

References

1. Yazıcı M, Celebi S, Kuzdan Ö, Koçan H, Ayyıldız HS, Bayrak İK, Bilgici MC, Yapıcı O, Kefeli M, Arıtürk E. Current radiological techniques used to evaluate unilateral partial ureteral obstruction: an experimental rabbit study. Int Urol Nephrol 2015;47:1045-50.
2. Groshar D, Wald M, Moskovitz B, Issaq E, Nativ O. Quantitative SPECT of 99mTc-DMSA uptake in kidneys of infants with unilateral ureteropelvic junction obstruction: assessment of structural and functional abnormalities. J Nucl Med 1999;40:1111-5.
3. Khalil KI, Shokeir AA, Wafa EW, Gad Gel-M, Helmy SA, Nour EM, Sarhan M. Renoprotection against complete unilateral ureteric obstruction: Is there an ultimate choice? Arab J Urol 2012;10:199-206.
4. Zhao CL, Yang WZ, Zhou HY, Ma T. Effects of ureteral obstruction on intrapelvic pressure and renal function. J Hebei Med Coll Contin Educ 2007;24:12-3, 19.
5. Wang CY, Yang QS, Gao C, Muhemmet, Li S, Jiang LL, et al. Variation features of basic glomerular filtration

function in experimental rabbits with partial unilateral ureteral obstruction. J Pract Med 2016;32:2283-87.
6. Lee WG, Kim JH, Kim JM, Shim KM, Kang SS, Chae HI, Choi SH. Renal uptakes of 99mTc-MAG3, 99mTc-DTPA, and 99mTc-DMSA in rabbits with unilateral ureteral obstruction. In Vivo 2010;24:137-9.
7. Ma S, Ye Z and Chen Z. Changes of glomerular filtration rate in partial unilateral ureteral obstructive kidney of rabbits. Med J Wuhan Univ 2006;27:399-401,405.
8. Yang GT, Yang JJ, Yao MY. Renal dysfunction and tubulointerstitial fibrosis caused by partial unilateral ureter obstruction. Journal of Southeast University 2005;24:339-43.
9. Claesson G, Svensson L, Robertson B, Josephson S, Cederlund T. Experimental obstructive hydronephrosis in newborn rats. XI. A one-year follow-up study of renal function and morphology. J Urol 1989;142:1602-7.
10. Barthez PY, Smeak DD, Wisner ER, DiBartola SP, Chew DJ. Ureteral obstruction after ureteroneocystostomy in dogs assessed by technetium TC 99m diethylenetriamine pentaacetic acid (DTPA) scintigraphy. Vet Surg 2000;29:499-506.
11. Provoost AP, Van Aken M, Molenaar JC. Sequential renography and renal function in Brown-Norway rats with congenital hydronephrosis. J Urol 1991;146:588-91.
12. Dissing TH, Eskild-Jensen A, Mikkelsen MM, Pedersen M, Frøkiaer J, Djurhuus JC, Gordon I. Normal differential renal function does not indicate a normal kidney after partial ureteropelvic obstruction and subsequent relief in 2-week-old piglets. Eur J Nucl Med Mol Imaging 2008;35:1673-80.
13. Ajmi S, Ben Ali K, Guezguez M, Sfar R, Nouira M. Captopril renography as a prognostic factor in obstructive hydronephrosis with preserved renal function. Rev Esp Med Nucl 2010;29:20-4.
14. Moon DH, Park YS, Jun NL, Lee SY, Kim KS, Kim JH, Yoon CH, Kang W, Lee HK. Value of supranormal function and renogram patterns on 99mTc-mercaptoacetyltriglycine scintigraphy in relation to the extent of hydronephrosis for predicting ureteropelvic junction obstruction in the newborn. J Nucl Med 2003;44:725-31.
15. Inanir S, Biyikli N, Noshari O, Caliskan B, Tugtepe H, Erdil TY, Akpinar I, Kiyan G, Alpay H. Contradictory supranormal function in hydronephrotic kidneys: fact or artifact on pediatric MAG-3 renal scans? Clin Nucl Med 2005;30:91-6.
16. Khan J, Charron M, Hickeson MP, Accorsi R, Qureshi S, Canning D. Supranormal renal function in unilateral hydronephrotic kidney can be avoided. Clin Nucl Med 2004;29:410-4.
17. Maenhout A, Ham H, Ismaili K, Hall M, Dierckx RA, Piepsz A. Supranormal renal function in unilateral hydronephrosis: does it represent true hyperfunction? Pediatr Nephrol 2005;20:1762-5.
18. Gates GF. Split renal function testing using Tc-99m DTPA. A rapid technique for determining differential glomerular filtration. Clin Nucl Med 1983;8:400-7.
19. Gates GF. Glomerular filtration rate: estimation from fractional renal accumulation of 99mTc-DTPA (stannous). AJR Am J Roentgenol 1982;138:565-70.
20. Gates GF. Computation of glomerular filtration rate with Tc-99m DTPA: an in-house computer program. J Nucl Med 1984;25:613-8.
21. Gates GF. A dose-attenuation shield for use in glomerular filtration rate computations. A method for combined renal scintiangiography and functional quantification. Clin Nucl Med 1991;16:73-8.
22. Rehling M1, Jensen JJ, Scherling B, Egeblad M, Lønborg-Jensen H, Kanstrup I, Dige-Petersen H. Evaluation of renal function and morphology in children by 99mTc-DTPA gamma camera renography. Acta Paediatr Scand 1989;78:601-7.
23. Toyoshima S, Noguchi K, Seto H, Shimizu M, Watanabe N. Functional evaluation of hydronephrosis by diffusion-weighted MR imaging. Relationship between apparent diffusion coefficient and split glomerular filtration rate. Acta Radiol 2000;41:642-6.
24. Piao S, Park J, Son H, Jeong H, Cho SY. Evaluation of renal function in patients with a main renal stone larger than 1 cm and perioperative renal functional change in minimally invasive renal stone surgery: a prospective, observational study. World J Urol 2016;34:725-32.
25. Suda K, Koga H, Okawada M, Doi T, Miyano G, Lane GJ, Yamataka A. The effect of preoperative urinary tract infection on postoperative renal function in prenatally diagnosed ureteropelvic junction obstruction: Indications for the timing of pyeloplasty. J Pediatr Surg 2015;50:2068-70.
26. Cheng MH, Zeng FW, Xie LJ, Li JF, Zhang F, Jiang H. A new quantitative method for estimating glomerular filtration rate and its clinical value. Clin Physiol Funct Imaging 2016;36:118-25.
27. Zhao CL, Cai WQ, Huo HX. Experimental study on renal functional reversibility in rabbits after relieving the acute ureteric obstruction. Chinese Journal of Surgery

2005;43:1480-1.
28. Schweitzer FA. Intra-pelvic pressure and renal function studies in experimental chronic partial ureteric obstruction. Br J Urol 1973;45:2-7.
29. Fink RL, Caridis DT, Chmiel R, Ryan G. Renal impairment and its reversibility following variable periods of complete ureteric obstruction. Aust N Z J Surg 1980;50:77-83.
30. Parida GK, Tripathi M, Kumar K, Damle N. Objective improvement in renal function post-Dietl's crisis: Documented on renal dynamic scintigraphy. Indian J Nucl Med 2016;31:240-1.
31. Aziz MA, Hossain AZ, Banu T, Karim MS, Islam N, Sultana H, Alam MI, Hanif A, Khan AR. In hydronephrosis less than 10 % kidney function is not an indication for nephrectomy in children. Eur J Pediatr Surg 2002;12:304-7.
32. Kampa N, Wennstrom U, Lord P, Twardock R, Maripuu E, Eksell P, Fredriksson SO. Effect of region of interest selection and uptake measurement on glomerular filtration rate measured by 99mTc-DTPA scintigraphy in dogs. Vet Radiol Ultrasound 2002;43:383-91.
33. Westgren F, Ley CJ, Kampa N, Lord P. Effects of hydration on scintigraphic glomerular filtration rate measured using integral and plasma volume methods in dogs with suspected renal disease. Vet Radiol Ultrasound 2014;55:632-7.

Cite this article as: Yang Q, Wang C, Gao C, Maimaiti W, Li S, Jiang L, Shen M, Shen Y. Does baseline renal function always decrease after unilateral ureteral severe obstruction?—experimental validation and novel findings by Tc-99m diethylene triamine pentaacetate acid (DTPA) dynamic renal scintigraphy. Quant Imaging Med Surg 2019;9(8):1451-1465. doi: 10.21037/qims.2019.07.09

